

The application of Feedforward Transmit Diversity to a system with Adaptive Modulation and Coding

D.D.N Bevan, C.R. Ward and W. Tong
Nortel Networks

Abstract-This paper examines the potential benefits of employing downlink Feedforward Transmit Diversity (FF-TxD) in wireless systems which utilise Adaptive Modulation and Coding. Instead of employing FF-TxD in such a system, the results presented suggest that multiple Node B transmit antennas could better be utilised to implement a spatial processing technique which exploits parallelism in the MIMO channel, such as one of the recently-proposed Space-Time Coding schemes

both paths have to be deeply faded before we see a significant reduction in CNIR at the output of the STTD Rx Processor. Similarly, going from a 1:2 baseline to 2:2 STTD we go from 2-way to 4-way diversity, but with no change in *mean* CNIR.

I. INTRODUCTION AND SYSTEM MODEL

This paper investigates the potential benefits of employing dual transmit antenna downlink Feedforward Transmit Diversity (FF-TxD) schemes, such as Space-Time Transmit Diversity (STTD)[1][2], in wireless systems which utilise Adaptive Modulation and Coding (AMC). One such system would be the downlink of the recently-proposed 'High Data Rate' (HDR) system for low-mobility (nomadic) Wireless Internet Access [3]. We will assume the system is operating in a multiple-input-multiple-output (MIMO) channel with an impulse response on each transmit (Tx) to receive (Rx) path which is flat in frequency (i.e. non-dispersive). Furthermore, we will assume a Quasi-static block Small-Scale Fading (SSF) model, such that the complex channel coefficients don't change over a coded block, and take independent random (Rayleigh distributed) values from block to block, and from Tx-Rx path to Tx-Rx path. The link model is shown in Fig. 1, where we consider N_T transmit antennas (where $N_T=1$ or 2) at the Base Station ('Node B') and N_R receive antennas (where $N_R=1, 2$ or 4) at the User Equipment (UE). At each UE antenna, we assume that the STTD receiver processing is as described in [1][2]. When multiple UE antennas are employed (four are shown in Fig. 1), then the process by which the multiple branches are combined in the UE Rx is assumed to be the Maximum Ratio Combiner (MRC) diversity reception technique [4].

II. ANALYSIS

A. Transmit and Receive Diversity

In effect, what a dual-Tx-antenna FF-TxD scheme such as STTD offers (compared to a single-Tx-antenna baseline) is a doubling in the order of diversity of the Node B-to-UE link. However, this diversity improvement is obtained without providing any improvement to the *mean* Carrier-to-Noise-plus-Interference Ratio (CNIR). In general, it can be shown [1 Section V] that STTD with two transmit and N_R receive antennas is equivalent in its fading characteristics (after appropriate normalisation of the mean CNIR) to MRC with one transmit and $2 \times N_R$ receive antennas. Thus going from an $N_T:N_R = 1:1$ baseline to 2:1 STTD we go from 1-way to 2-way diversity. In simple terms, we have two effective transmission paths, and the diversity behaviour means that

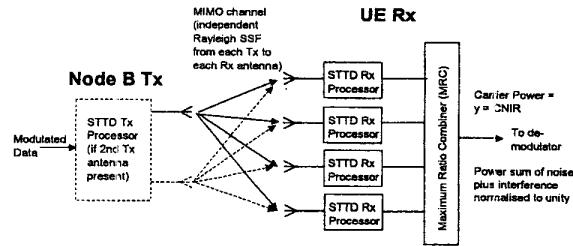


Fig. 1 STTD Link Model

B. Fading Distributions

In order to quantify the benefit of an increase in diversity in a system with AMC, we need to model the SSF distributions involved. Consider first the case where $N_T:N_R = 1:1$. Since we are assuming Rayleigh fading on the Tx-Rx path, it can be shown that the probability distribution function (pdf) of the CNIR at the UE is centrally χ^2 ('chi-squared') distributed with 2 degrees-of-freedom (d.o.f.) [5 eqn. 2-1-126]. Either a doubling of the number of transmitter antennas, or a doubling of the number of receiver antennas (with appropriate renormalisation of CNIR) will change the post-MRC-combining CNIR distribution to χ^2 with 4 d.o.f. A further doubling of the order of diversity (i.e. doubling again the number of Tx or Rx antennas) gives 4-way diversity, and hence a CNIR distribution which is χ^2 distributed with 8 d.o.f. In general, it can be shown [5 p.781] that for $N_T=1$ the CNIR distribution at the output of the MRC combiner is χ^2 with $2 \times N_R$ d.o.f. It follows from the above that if $N_T=2$ then the CNIR distribution at the output of the MRC combiner is χ^2 with $4 \times N_R$ d.o.f.

In general, the central χ^2 distribution with n d.o.f., $p_Y(y)$, which represents the pdf of the sum, Y , of the squares of n i.i.d. gaussian random variables each with zero mean and variance σ^2 can be represented as follows [5 eqn. 2-1-110]:

$$p_Y(y) = \frac{1}{\sigma^n 2^{n/2} \Gamma(n/2)} y^{n/2-1} \exp\left(\frac{-y}{2\sigma^2}\right) \quad (1)$$

where $\Gamma(p)$ is the gamma function (see [5 eqn. 2-1-111]).

All of the analysis presented herein was conducted numerically, using the mathematical software program Mathcad. This contains a function '*dchisq(y,n)*', which generates a χ^2 pdf of y , with n d.o.f. and $\sigma^2=1$. The output of

this function, for $n=2,4,8$ is shown in Fig. 2. That this is consistent with (1) can be verified by direct comparison of Fig. 2 with [5 Fig. 2-1-9].

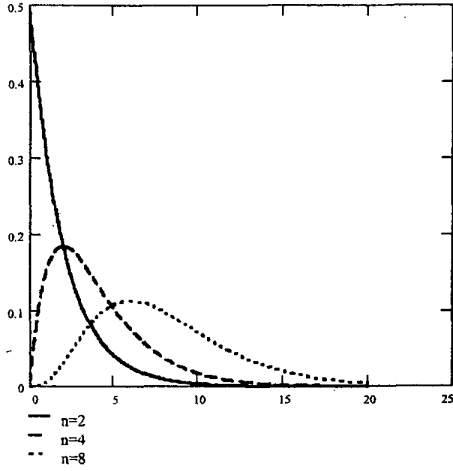


Fig. 2 Central chi-squared probability distribution function for n d.o.f., as plotted by Mathcad

The curves of Fig. 2 can be used to represent the distribution of the CNIR, y , at the output of the MRC combiner in Fig. 1. However, we need to apply appropriate normalisation to each of these curves if we wish to compare performance with different levels of diversity (i.e. different antenna configurations) at the *same* mean CNIR. We assume (without loss of generality) in Fig. 1 that the MRC weights are normalised to give unity noise-plus-interference power at the MRC combiner output. Thus the quantity y represents *both* post-MRC-combiner carrier power *and* post-MRC-combiner CNIR. If the pdf of y is denoted $p_Y(y)$, then the *mean* power in y , denoted $P_{_y}$, is given by [5 eqn. 2-1-61]:

$$P_{_y} = E(y) = \int_{y=0}^{y=\infty} y \cdot p_Y(y) dy \quad (2)$$

where $E(\bullet)$ denotes expectation, and y takes on only positive values (since it represents a power). Furthermore, since $p_Y(y)$ represents a pdf, it must of course also satisfy the condition

$$\int_{y=0}^{y=\infty} p_Y(y) = 1. \quad (3)$$

The curves of Fig. 2 represent the post-MRC-combiner carrier power or CNIR distributions for 1-way, 2-way and 4-way diversity. However, they each have a different mean power, since they are the distribution of the power sum of 2, 4 and 8 i.i.d. unity variance gaussian random variables respectively. Thus we first renormalise them to unity mean CNIR by computing the functions ' $n.dchisq(n,y,n)$ '. These are plotted in the curves of Fig. 3 for $n=2,4,8$. It is easy to verify that the curves of Fig. 3 satisfy (3), and also satisfy (2) for $P_{_y}=1$. By comparison of Fig. 2 and Fig. 3 it can be seen that

the normalisation has been achieved in each case by appropriate compression of the horizontal axis, and extension of the vertical axis, as occurs through transformation (or normalisation) of a random variable [5 Fig. 2-1-4].

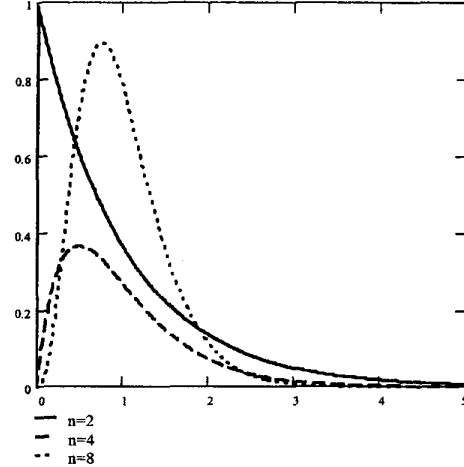


Fig. 3 Central chi-squared probability distribution function for n d.o.f., normalised to unity mean

As stated above, the curves of Fig. 3 are normalised to unity mean carrier power (or unity mean CNIR), such that $P_{_y}=1$. We can further renormalise to *any* arbitrary mean CNIR, $P_{_y}$, (through appropriate expansion or compression of the horizontal and vertical axes), as long as we ensure that (2) and (3) are still satisfied.

It can be seen from Fig. 3 that as the order of diversity increases, the distribution of CNIR at the MRC combiner output becomes narrower. Ultimately, when the order of diversity is very high, we will approach a distribution of CNIR which is an impulse centred on $y=1$. This impulse pdf also represents the pdf of post-MRC-combiner CNIR in a static (nonfading) channel.

C. Link bit loading

In the previous section we have discussed the distribution of CNIR at the MRC combiner output, due to the combination of the phenomenon of Small-Scale Fading, and the operation of the transmit and receive diversity processing. We stated earlier that we are considering a system with AMC, such that the *instantaneous* 'bit loading' (i.e. 'spectral efficiency' or 'link throughput'), is continually adapted such that it is always optimised, and thus 'tracks' the SSF. We shall represent the bit loading in units of information-bits-per-symbol (denoted 'bpsl'). It can readily be seen that given our Quasi-static SSF link model described earlier, the AMC must adapt at the block rate. Exactly how this AMC is implemented in practice is beyond the scope of this paper, but we assume that there is some fast feedback channel on the uplink between the UE Rx and Node B Tx. This allows the UE to signal to the Node B on a block-by-block basis a

desired bit loading based on measurements of CNIR (see, for example, [3]).

How do we calculate the bit loading for any arbitrary instantaneous CNIR? For ease of analysis, we will assume a system using 'Shannon' (noise-like) encoding [6], and 'long' coding blocks which achieve a bit loading that approaches the Shannon rate with negligible block or bit error probability. Thus, the characteristic of bit loading versus instantaneous CNIR is given as follows [6 eqn. (29)]:

$$C_S = \log_2(1 + CNIR) = \log_2(1 + y) \quad (4)$$

This characteristic is plotted in Fig. 4 (against a decibel measure of CNIR), where we note that at an instantaneous CNIR of 0dB we can achieve a bit loading of 1 information bit per modulation symbol. At a CNIR of 10dB, we can achieve a bit loading of almost 3.5 bpsl.

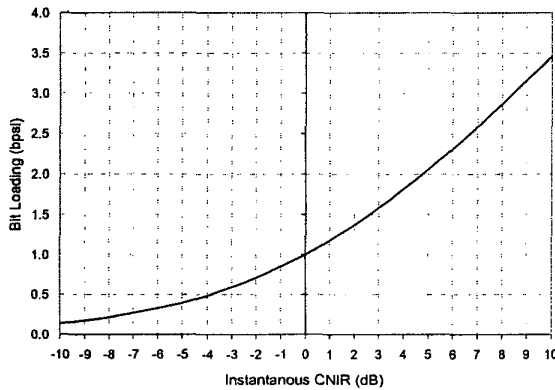


Fig. 4 Assumed instantaneous bit loading characteristic (per Shannon [6])

Of course in practice our block length will be much shorter than the long coding blocks assumed by Shannon, and our codes will be 'real-life' (with constrained encoding and decoding complexity) and thus they will not achieve the Shannon bit loading of (4). However, experience shows that even if real-life codes fall some 1-4dB short of Shannon at a bit error ratio of 10^{-6} , they will still have a performance in terms of bit loading versus CNIR which closely tracks the Shannon curve (i.e. lies parallel to it). Therefore, even though the *absolute* bit loading numbers generated by this analysis may be optimistic (versus instantaneous CNIR) by 1-4dB or so, the trends should be closely matched in real life.

D. Calculation of mean bit loading

In the above sections we have discussed the fading distributions, both within the MIMO channel and at the output of the UE Rx processor. We have also discussed what bit loading can be achieved at any given *instantaneous* post-MRC-combiner CNIR. We now wish to compute the *mean* bit loading, averaged over the SSF, for any given diversity order at any given mean CNIR. The analysis technique we employ is, for each order of diversity and for each value of *mean* (expected) CNIR, to integrate the bit loading over the

appropriately-normalised distribution of the fading of CNIR. Thus, expressed mathematically, if y represents the instantaneous CNIR with appropriately normalised pdf $p_Y(y)$, and $C_S(y)$ represents the bit loading which can be achieved for an instantaneous CNIR of y , then the *mean* bit loading, which we shall denote C_{SSF_y} , is given by:

$$C_{SSF_y} = E(C_S(y)) = \int_{y=0}^{y=\infty} C_S(y) \cdot p_Y(y) dy \quad (5)$$

Equation (5) gives the mean bit loading for a given diversity order and for a given mean CNIR at the MRC combiner output. The solution can be computed numerically, using Mathcad, for a range of different mean CNIRs and diversity orders. The results of such an analysis are presented below.

III. RESULTS

The results of the numerical computation of (5) for a range of mean CNIRs (0dB to 20dB) and diversity orders (1,2 and 4) are presented in Fig. 5. Also shown is a curve for the 'static case'. This is the case where the CNIR at the MRC combiner output is nonfading, and so the instantaneous bit loadings and the mean bit loading are identical. It can be seen that the curve for the static case in Fig. 5 is identical to that in Fig. 4.

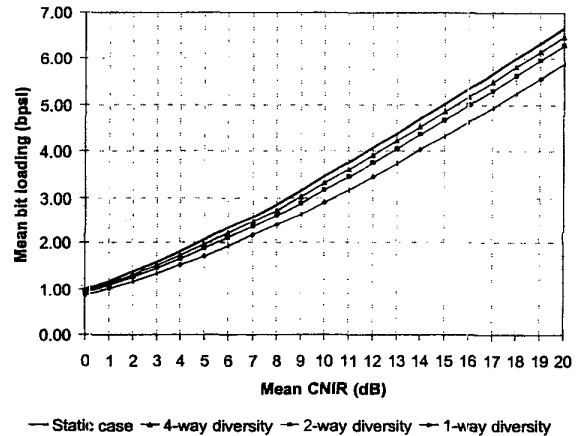


Fig. 5 Mean bit loadings as a function of mean CNIR for various diversity orders, assuming independent Rayleigh Small-Scale Fading and AMC with Shannon bit loading

It can be seen from Fig. 5 that the curves for 1-way, 2-way and 4-way diversity closely track the static curve, with an offset of approximately 2dB, 1dB and 0.5dB respectively. Thus, in going from 1-way to 2-way diversity in such an AMC system we obtain about 1dB of what we could term 'diversity gain'. Therefore in going from an $N_T:N_R = 1:1$ baseline to 1:2, we would obtain about 1dB diversity gain, in addition to the 3dB gain in *mean* CNIR that MRC would offer [4]. However, when we then further enhance the system by going from 1:2 to 2:2 with FF-TxD (e.g. STTD), there is

no extra CNIR gain, and the additional diversity gain we achieve will only be around 0.5dB or so. In terms of mean bit loading this 0.5dB diversity gain translates to less than 5% increase over the whole range of mean CNIRs from 0dB to 20dB. Even infinite-way diversity (i.e. the static case) would at best offer barely more than 10% mean bit loading increase compared to the 2-way diversity case over the range of mean CNIRs investigated. Thus, the opportunities for mean bit loading improvements solely through the application of FF-TxD in such a system are somewhat limited.

IV. CONCLUSIONS

The results of Fig. 5 provide a strong argument for eschewing the use of FF-TxD in the downlink of an AMC-based system such as HDR, in the low-mobility (low Doppler) frequency-flat channel scenario investigated here. We suggest instead that if we have two transmit antennas available for the downlink, we could better utilise them by choosing a more sophisticated spatial processing technique. Candidate techniques could be those which promise significantly greater gains through exploitation of *parallelism* in the MIMO channel, such as one of the recently-proposed Space-Time Coding schemes (discussed in [7]).

REFERENCES

- [1] S.M. Alamouti, "A Simple Transmit Diversity Technique for Wireless Communications", *IEEE Journal on Sel. Areas in Comm.*, Vol. 16, No. 8, October 1998, pp. 1451-1458
- [2] TI Company, "Space Time Block Coded Transmit Antenna Diversity for WCDMA" *SMG2 document 581/98*, submitted 30 October 1998
- [3] P. Bender, P. Black, M. Grob, R. Padovani, N. Sindhushayana and A. Viterbi, "CDMA/HDR: A Bandwidth-Efficient High Speed Wireless Data Service for Nomadic Users", *IEEE Communications Magazine*, July 2000, pp. 70-77
- [4] D.G. Brennan, "On the Maximum Signal-to Noise Ratio Realizable from Several Noisy Signals", *Proceedings of the IRE*, vol. 43, October 1955, p. 1530
- [5] J.G. Proakis, *Digital Communications*, McGraw-Hill, Third Edition, 1995
- [6] C.E. Shannon, "Communication in the Presence of Noise", *Proc. IRE*, vol. 37, Jan. 1949, pp. 10-21
- [7] D.D.N. Bevan, R. Tanner and C.R. Ward, "Space-Time Coding for Capacity Enhancement in Future-Generation Wireless Communications Networks", *IEE Colloquium on Capacity and Range Enhancement Techniques for the Third Generation Mobile Communications and Beyond*, Digest No. 00/003, February 2000, pp. 8/1-8/11